CALCULATION STUDY OF HELICOPTER ELASTIC ROTOR BLADE DEFORMATION IN PLANES OF PULL, ROTATION AND TORSION BY METHOD OF FORTH INTEGRATION

V.A. Ivchin
MIL Moscow Helicopter plant, JSC
Russia

I.O. Averyanov
"MATI" - Russian State Technological University
Russia

OVERVIEW

Russian State Technological University (MATI) jointly with MIL Moscow Helicopter plant, JSC has developed a generic calculation method of loading and strength of rotorcraft flight structure that operates in transient regimes of flight. The given method makes it possible to define the results of calculation for the whole range of tasks considered in the design of rotorcraft flight structure that causes safety and reliability growth of this type of aircrafts.

To achieve this objective the study has been conducted to investigate the possibility of applying the method of forth integration with respect to the system of equations of the blade deformation working in the field of centrifugal forces and taking into account its joint fluctuations in the planes of thrust, rotation and torsion. Application of this approach allowed to solve this system of equations with a high degree of accuracy.

Based on the study established the methodology and algorithms to meet the challenges on the definition the loading and strength of rotor blades operating in transient regimes of flight and to determine the rotor blade characteristics with the ability to set the boundary of time-changing conditions.

To evaluate the performance of the developed methods and calculation algorithms a number of problems, solutions, results are compared with the well known solutions and experimental data. Fundamentals and the results of the research are presented in this article.

1. INTRODUCTION

At present there are a number of reliable methods that have been developed to calculate the loading of the rotorcraft flight structure in stationary regimes. A great contribution to this field was made by Russian experts Grodko L.N. Nekrasov A.V., Myagkov Y.A., Liss A.Y., Burtsev B.N., Mikhailov, S.A. and others. An example of the application program for the calculation of loads on the rotor blades is the program for calculating the characteristics of rotors designed by A.V. Nekrasov.

However, most of the existing calculation methods deal with stationary helicopter flight regimes where the equations of deformation of the blades are partial differential equations with periodic coefficients. To solve these equations a well-proven method of Bubnov-Galerkin is used. In the solving a similar problem for the transition and maneuver regimes most authors also use this method on the basis of quasi-static approach. Such approach for calculating the loads on the rotorcraft flight structure for maneuvering regimes is very rough.

There are other regimes calculated for the rotor and antitorque rotor blades, which are also not periodic, for example, the blade strikes on the mechanical stops in the wind in the parking lot and maneuvers, in the unwinding of rotors in a gust of wind, and so on.

New proposals appear for the construction of a rotorcraft flight structure. V.M. Pchelkin at "MIL Moscow Helicopter plant", JSC in 1991 proposed a new scheme of rotorcraft flight structure to reduce the load on the single-rotor helicopter control system, called SLES (Stall Local Elimination System), see [1]. In 2007 this system has been

proposed by N.S. Pavlenko for high-speed helicopter [2, 3]. This method is based on restraint of the blade in a horizontal hinge, depending on its azimuthal position.

The most appropriate approach for the calculation of transient regimes of flight and new design solutions in the field of rotorcraft flight structures is the use of methods of forth integration of the deformation based on the finite-difference scheme. This article presents some results of the development of algorithms and program for solving the problem of determining the elastic blade deformation regarding its torsion and bending in two planes.

The main design formulas for the elastic bending in the plane of thrust and rotation and the helicopter rotor blades torsion are equations derived by A.Y. Liss [4].

The article also presents the results of comparative calculations of rotor blade natural frequencies that were obtained by the proposed method and the Bubnov-Galerkin method, and examples of calculations of some problems that change the boundary conditions of fixing of rotor blade butt during the transient regime.

2. MATHEMATICAL ROTOR MODEL

2.1 Problem solving method

We considered the equations of deformation of the blade [4], describing its joint fluctuations in the planes of thrust, rotation and torsion. In general, these equations are written in the form of equations (1):

$$\begin{aligned} A_1 + \ddot{B}_1 &= F_1 \\ A_2 + \ddot{B}_2 &= F_2 \\ A_3 + \ddot{B}_3 &= F_3 \end{aligned} \qquad (1)$$

where Ai, Bi are linear integro-differential operators on functions x(r,t), y(r,t), and θ (r,t). Here, r - radius of the blade, t - time, the dot denotes the partial derivative with respect to time.

In the system (1) index 1 denotes an equation relating to the deformation in the plane of rotation, index 2 - equation relating to deformation in the plane of thrust, and index 3 denotes an equation relating to the torsion of the blade. Formulas that reveal the values of A_i, B_i, and F_i, taking into account the first order of smallness, are presented in the [4]. The values of A_i, B_i depend only on the unknown quantities of deformation of the blade *x, y,* θ and their derivatives with respect to the radius. The inertial terms, which expressions contain first time derivatives, and some inertial and terms that are quadratic with respect to deformations that are not negligible are included in the expressions for F_i. It also includes external aerodynamic loads.

The essence of the method used is to present the study of the differential equation in the form of the difference scheme and reduce it to a linear equation. To solve the differential equations of deformation of the blades the finite difference method is used. This method is described in [5, 6]. Solution of the system of deformation (1) allows us to define movements and twisting of the blade section under consideration. If we consider all sections of the blade of all rotor blades simultaneously, we can define the distorted condition of the rotor blades at any point of time. This fact allows us to renounce the use of the averaged of rotor thrust turnover that allows us to simulate all flight regimes. On the basis of this method the RNV program was developed that allows modeling the work of the rotor blade in the transient flight regimes.

Solving the system of equations (1) with zeroed right-hand sides, and considering all the sections of one blade, we find the solution to determine the characteristics of its own motion. Using algorithms of spectral analysis, based on this method the SCH program was developed. The program allows solving problems of determining of the blade natural modes and frequencies.

2.2 Boundary conditions

One of the significant advantages of the developed method is the possibility of modeling a wide variety of boundary conditions, including changing over the turnover of the rotor, that is especially important due to new concepts for rotorcraft flight structures [1, 2, 3], which cannot be calculated by the traditional methods.

The study covered the following types of fixation of blade to the hub: rigid fixation, hinged fixation [6, 7], hinged fixation with a clamping of the blade at

certain azimuths (blade operation in the SLES system [7]), a variable hinge - rigid fixation (in the modeling of the fall of the blade to stop overhang [7]).

2.3 Aerodynamic rotor blade model

We used an aerodynamic element model of the rotor blade Mi-8, in which aerodynamic loads on the blades were calculated for each section of the blade in accordance with the calculated values of the angles of attack and Mach numbers [8]. The rotor blade sections are made with the sectional profile NACA-230. The performance profiles were obtained in a wind tunnel for the entire operating range of speeds and regimes of helicopter flight.

The distribution of inductive velocities over the disk of the rotor blade was calculated on the basis of the traditional theory of Glauert-Lock linear distribution and more accurate Mangler - Squire disk theory.

3. PERFORMANCE EVALUATION OF THE METHOD AND ALGORITHMS FOR CALCULATION

3.1 Test problems

To evaluate the performance of the developed method and algorithms a number of tests was carried out, gradually increasing complexity of calculations. Their solutions were compared with exact solutions, solutions obtained by using FEM analysis, and solutions obtained by other authors.

3.1.1 Fluctuations of non-rotating cantilever beam

Originally a classical problem has been solved, which has an exact analytical solution. This task was considered cantilever beam of constant cross section that makes free vibrations in one plane. The obtained results were compared with the exact solutions [9]. The calculation results (for some sections) and the graphics of natural modes and frequencies are shown in Figure 1 and Figure 2.

3.1.2 Fluctuations of non-rotating blade

The following problem regards free bending vibrations of rigidly fixed, non-rotating blade of the helicopter Mi-8 in two planes. The results are compared with the results obtained by finite element method with the help of the MSC Nastran package.

3.1.3 Fluctuations of the rotating blade

Then we considered the problem, which deals with fluctuations of the rotating blade of Mi-8 in the plane of thrust. The calculation results were compared with the results obtained by A.V. Nekrasov. In the calculations we used elastic-mass characteristics of the blade identical to that of the compared task.

3.1.4 The study of joint bending-torsion vibration

This problem considers rotating blade vibrations in the planes of thrust and rotation, and elastic torsional deformation of the blade. The calculation results are compared with the results obtained by A.Y. Liss. For more adequate comparison we used elastic-mass characteristics of the blade, the same as in the problem solved by A.Y. Liss.

3.1.5 Estimated results

Evaluation of the solutions obtained in sections 3.1.1 - 3.1.4 is presented in Table 1. According to the results of comparisons, we can conclude that the results of calculations performed by the proposed method are well converged with the exact solutions and calculations made by other authors.

Table 1. Comparison the result of analysis with known solutions

№ tones	Compared solution, 1/sec	Solution obtained, 1/sec	Relative deviation
3.1.1 Fluctuations of non-rotating cantilever beam			
1	3.94	4.0	0.02
2	24.68	24.0	0.03
3	69.10	67.0	0.03
4	135.44	129.0	0.05
3.1.2 Fluctuations of non-rotating blade			

1st tone. Plane of thrust	3.91	4.0	0.02
1st tone. Plane of rotation	10.13	10.0	0.01
3.1.3 Fluctuations of the rotating blade			
1	21.22	21.0	0.01
2	54.50	54.0	0.01
3	93.30	92.0	0.01
4	147.42	142.0	0.04
3.1.4 Joint flexural-torsional vibrations/oscillations			
Plane of thrust			
2	20.41	20.0	0.02
3	53.45	52.0	0.03
5	93.39	87.0	0.07
Plane of rotation			
1	5.51	6.0	0.08
3	53.45	52.0	0.05
Plane of torsion			
6	152.56	153.0	0.01
7	160.10	157.0	0.02

3.2 Modeling of steady-state flight regimes

After the test calculations, we calculated a number of stationary flight regimes of Mi-8. Calculations were performed taking into account the elastic deformation and movement of the blades in the horizontal and vertical planes with respect to the vertical and horizontal hinge, and torsion deformation of the blades.

3.2.1 Horizontal flight regime

The modeling results of horizontal flight regime in the developed program were compared with the existing solution to this problem, obtained by a different method [4]. Therefore, all the relevant characteristics of the regime correspond to the characteristics of the existing solution: the five-blade rotor Mi-8 helicopter; free-stream velocity 230 km/h, rotor attack angle -3.4°; rotor angular velocity 20.106 rad/sec. Elastic-mass characteristics of the blade were used interpolated from the existing data source, due to the increased number of calculated cross sections. At the initial time the blades were in the plane of rotation, the value of induced velocity of the rotor was assumed to be zero. In Figure 3 - Figure 6 some results of calculations are presented.

As seen from the graphs of the movement of the blade around the flapping and the feathering hinge the regime is set after the 2nd turn of the rotor. The motion of the blade relative to the drag hinge is stabilized after the 12th turn of the rotor. This is due both to the different natural frequencies of blades movement around the hinges, and with distinction in the aerodynamic damping. For the motion of the blades around the flapping hinge aerodynamic damping is much larger than the damping of the blades in the plane of rotation.

The obtained average value of rotor thrust for a turnover of 11 698 kg. According to the obtained displacement of blade sections we computed values of constant and variable moments and stresses. The results showed that the developed algorithm of calculation allows to determine the stress strain state in each section of the blade and the value of a rotor thrust at each given moment of time. This fact allows us to renounce the use of average turnover for the aerodynamic characteristics of the rotor as it was done in the comparable problem [4]. This fact will improve the accuracy of the calculations.

3.2.2 Hover regime

Then hover regime was calculated. In the absence of ready-made solution for this problem a qualitative assessment of the solution was carried out. Speed was assumed to be 0 km/h, the attack angle of the rotor was 0°, the angular velocity of the rotor rotation was 20.106 rad / sec and the angles of the swash

plate slope were 0°. In the initial position the blade was in the plane of rotation.

The calculation results are shown in Figure 7 - Figure 10. From these graphs we can see that the deformation of the blade in the plane of thrust and torsion, as well as the rotor thrust take constant value after the second rotation of the rotor blade. The deformation of the rotor blade in the plane of rotation takes place after the10th turn. The solution corresponds to the existing theories and results of flight tests.

According to the result of the considered problems of transient regimes we can conclude that the developed method for calculating of the rotor blades shows reliable results and is applicable for the calculation of stationary flight regimes.

4. MODELING OF FLIGHT TRANSIENT REGIMES

For preliminary estimates of loads on the rotor blade the "Gorkal" [10] regime has been selected, since the implementation of this maneuver in a helicopter with high overload leads to a significant stresses in the blades and an increase of loads in the helicopter control system. The task was to compare the load on the blade, calculated by forth integration and quasi-static method. For these calculations we used our program to provide the correct comparison of the results.

For the calculation of the dynamic regime we used the forth integration of the whole flight regime, taking into account the changes of operating control at each moment of time. Quasi-static calculation was performed with the averaging of all flight parameters and control actions in one revolution of the rotor, which was considered at some points of time. Quasi-static calculation is performed up to the convergence of flapping motion and deformation of the blade.

We regarded flight parameters obtained from the results of flight tests for Mi-24 as the initial data for our calculation, since the data for Mi-8 helicopters was not available. Although the designs of helicopters are different, the increment of control and flight parameters during the execution of regime can be used for computer modeling of Mi-8. The maneuver starts from the initial, balanced regime of level flight with the initial forward speed of 250 km/h. Transient regime is completed by a new steady-state regime at a flight speed of 145 km/h. Figure 11 - Figure 15 show the graphs of indicated air speed, attack angle, parameters of longitudinal and lateral control and the total flight time step, which were used to calculate the "Gorka" regime of Mi-8. Seven time-points were taken of the flight path of the transient regime for quasi-static calculation, where the characteristics of the flight regime and control system for one revolution of the rotor (which lies near the selected time-point) were averaged. The table lists the design parameters for quasi-static regimes.

Table 2. Table of parameters for calculations of quasi-static regimes

Time	1 sec	2 sec	3 sec	4 sec	6 sec	8 sec	12 sec
V, m/sec	67.73	61.31	53.62	43.98	32.18	43.98	41.17
χ, rad	0.039	-0.056	-0.051	-0.022	-0.01	-0.023	-0.009
η, rad	0.028	0.023	0.018	0.010	0.001	0.011	0.007
ϕ, rad	0.201	0.201	0.201	0.201	0.192	0.201	0.187
α, rad	0.167	0.343	0.096	-0.136	-0.085	-0.136	-0.126

Figure 16 and Figure 17 show some results of the calculations. Figure 16 shows a graph of rotor thrust change during the maneuver, and Figure 17 shows the values of sections deformation for the same period of time. The graph shows that the maximum average value of the rotor thrust reaches 19493 kg (0.85 sec), which corresponds to vertical overload.

$$n_y \approx 19493 / 10535 = 1.85$$

Figure 17 also shows a graph of displacement in the plane of the rotor thrust four separate sections of the blade located on the radii of 10.65 m, 8.35 m, 3.6 m and 3.8 m during the maneuver. It is evident that the movement of blade sections occurs with a frequency equal to the frequency of rotation of the rotor, while the vibration amplitude of the blade significantly increases in the interval of maximum overload for the maneuver. As can be seen from the graph of Figure 17 the maximum amplitude of vertical displacement is achieved at the end of the blade at a radius of 5.10 m. If during the final stationary regime the semi-range of vertical movement of the blade tip reaches ±0.5 m, the maximum value of the semi-range during the maneuver is ±2.25 m.

Further calculations of quasi-static regimes were performed in line with the data presented in Table 2. Comparative results of quasi-static and dynamic regimes for rotor thrust are shown in Table 3. Figure

18 - Figure 23 show the graphs of loads distributed over the blade.

Table 3. Table of results comparison: method of forth integration and quasi-static method

Time, sec		0	1	2	3	4	6	8	12
Rotor thrust, kg	Method of forth integration	10540	16521	15484	16722	13107	13819	14929	12814
	Quasi-static method	10535	17157	16543	16503	13110	13815	14799	12809

The variable component of moments of calculation by means of the forth integration method was defined in the time range of one turn of the rotor, the middle of which corresponded to the reported moment of time.

The graphs show the distribution of fixed and variable parts of the moments along the radius of blade at a moment of time equal to 2 sec for the two methods under consideration, as during this exact moment of time the difference between the compared approaches reaches its maximum. Blue lines on the figures show the results of quasi-static analysis, while red lines denote the results of the forth integration method.

Similar graphs were obtained for other regimes of calculation. The exceptions are the initial and final sections of the flight where the variable and constant parts of the bending and torsional moments are almost the same. In this case, the forth integration method gave a higher level of rotor blade loading.

Figure 24 shows the distribution of the maximum equivalent bending stresses along the radius of the blade that arises during the execution of the considered maneuver. The graph shows that the quasi-static approach for the calculation of maneuver and transient regimes gives understated values of the stresses in the blade. Stress analysis for this maneuver has shown that in the application of the quasi-static method the value of loads in the blade can be underestimated by 25%.

5. SOLUTION OF PROBLEMS IN THE DEFINITION OF BLADE INHERENT CHARACTERISITICS

5.1 The study of the blade inherent characteristics of Mi-8, hingedly suspended in the flapping hinge when it falls on the blade droop stop

This phenomenon may occur in the parking lot, when under the influence of wind gust loose blade rises and then drops when the wind dies down (this case is described in Section II-2 of NLGV). The fall of blade followed by its oscillatory motion, whose parameters may vary depending on the height of blade lift due to a gust of wind and its elastic-mass characteristics. To solve this problem to the equations of deformation of the blade the gravitational term was introduced, which was absent in the study [4]:

$$\Delta M_{изг} = \int_{r_*}^{R} m \cdot g \cdot (r - r_*) \cdot dr \qquad (2)$$

Originally blade droop was designed according to its static position on the block stop. Figure 25 presents the results of this calculation, obtained by the method proposed by the authors [6, 7].

The results were obtained by the pseudoviscosity method. In this method the aerodynamic damping was artificially increased by 100 times to reduce the estimated time. For greater clarity, the blade root shows the points corresponding to the virtual boundary conditions. Experimental values of the deflection of the blade tip of the Mi-8 helicopter is 1.15 m, and by calculation - 1.23m. The results well fit the exact solution of the formulas of the study [9]. The following calculation was performed for the dynamic regime of the blade fall to the stop without

damping aerodynamic forces. Figure 26 shows graphs with the blade deflection for four sections, Figure 27 shows the graph of the blade bending moment.

The results of analysis show that before the blade will be on the stop, it has a proper motion as a hinge blade, and after it goes on the stop it works as a fixed one. The blade oscillation frequency changes accordingly. It should be noted that as the blade movement increases the higher harmonics amplitude rise. This is due either to the blade load step change as it hits the stop, or comes off the stop. This kind blade load step change leads to a wide range of excitation frequencies, which, without damping, leads mainly to high-order harmonics.

Figures dashed lines show the blade tip average deflection and the blade butt average moment at in static (Figure 25). The graphs show that the blade proper motion gradually converges to oscillation with respect to the blade static position.

The next step was to analyze the influence of damping on the blades dynamics at fall to the stop. Figure 28 - Figure 29 show graphs of the blade four sections deflection and bending moment. The results show that the aerodynamic damping leads to the oscillation amplitude damping, though it is small and the decay time is relatively large. The graphs show that after the blade finally falls on the stop (t = 6-7 sec) high harmonics amplitudes significantly reduced, the damping stabilizes and the process converges to the static values.

In the absence of experimental data for the Mi-8 rotor blades, the task solution was compared with the experimental data for the other rotor blade (a composite one, with different elastic-mass characteristics).

The closest to the calculated cross section on the oscillogram is the one, marked as channel 1. Comparing the corresponding chart on the oscillogram for channel 1 with the bending moment calculated curve (Figure 30), we can observe good qualitative correspondence between the calculated and the experimental data. This allows us to conclude that the developed method is applicable for practical calculations of the rotor blade static characteristics.

5.2 The research of the Mi-8 rotor blade inherent characteristics operating in SLES

N.S. Pavlenko [2] at JSC "Mil Moscow Helicopter Plant. ML Mile" proposed a new concept of high-speed helicopter - SLES system (Stall Local Elimination System). This system is based on inventions by V.M. Pchelkin and N.S. Pavlenko in 1991 [1] to reduce loads on the single-rotor helicopter control system. This method is based on "pinching" blade in a flapping hinge, depending on its azimuthal position. Calculation of such a system represents a significant difficulty, since the boundary conditions of blade seal in the hub change during one blade revolution. The most plausible calculations based on the basis of a method of forth integration of equations with partial derivatives, developed by the authors [7]. Below are the results of the SLES blade natural mode study.

Originally we calculated the blade inherent characteristics with the hinge and stiff suspension. In contrast to the previous section, we consider a rotating rotor, the blades of which work in the centrifugal forces. . The rotational speed of the rotor corresponds to the nominal speed for the Mi-8 and is 20 1 / sec, the turnover period is 3.183 per sec.

Figure 31 shows a graph of the hinged blade natural modes and frequencies, while Figure 32 presents a diagram of the absolute values of tones' amplitude in accordance with the natural frequencies for a given blade, rounded to whole numbers to ease the comparison. The obtained results for natural frequencies converge with the exact solution given [9]. As can be seen from the graphs, zero and the first tone of the oscillations have the largest amplitude. Larger tone numbers have amplitude of fluctuations in 2 - 3 times smaller. Therefore, for the initial assessment it is reasonable to consider the lowest oscillation tones.

Figure 33 shows a graph of natural modes for rigidly fixed blade. Figure 34 presents a diagram of the absolute values of the amplitude of tones depending on the inherent frequencies for a given blade, rounded to whole numbers to ease the comparison. The results for natural frequencies coincide with the exact solution given [9].

It should be noted that the zero tone for hinged blade and tone 1 for a tough one have similar

characteristics in calculation values of the elastic-mass arrangement of Mi-8 blades.

Further, we calculated two variants of the rotorcraft flight structure configuration using the SLES concepts:

- Range of flapping hinge lock is 225°…315°;

- Range of drag hinge lock is 180°…360°.

Figure 35 and Figure 36 show graphs of natural vibrations and bending moments of the rotating blade in time for the first variant of hinge pinch in the range of azimuths 225°…315° for the calculation in the four radii.

Figure 37 shows the spectrum of natural frequencies of the blades in the presence of SLES on the rotor. which shows that the use of SLES substantially changes the frequency characteristics of blade, as compared to the hinge, and compared with a rigid blade. The graph also shows that there is a frequency close to the rigid and hinged to the blade, as well as the frequency resulting from a close of the natural frequencies of the two options for maintaining the blades to the hub. This reason is explained by the presence of oscillations of the beat, and as a consequence, high bending moments on the blades, the amplitude of the variable part of which reaches a value of ± 150 kgm.

The second version of the calculation, with a range of pinching 180°…360°, showed similar results. Figures 38 and 39 show the results of calculations of the carrier system SLES, which has a range of flapping hinge lock operation is 180°…360°. Figure 38 shows the change in deformation of certain sections of blade in the plane of thrust, while Figure 39 is the change of the bending moment on the four radii of the blade.

Figure 38 shows that the range of time Δt=0…0.22 the bending moment in the butt blade is equal to 0, because it works a horizontal hinge. At the time of pinching blade (t = 0.22 sec) begins to rise sharply bending moment in the butt of the blade, and by the time the release of blade in a horizontal hinge (t = 0.31sec, the rotor has made a 180°) its value reached a value of ~160 kgm. After the liberation of blade there is a peak load of the entire radius of the blade, which leads to a variable bending strains and stresses with a high frequency blade. Until next time pinching blade (t = 0.62 sec) caused oscillations with high frequency start to increase due to changes in peak loads on the blade when blade “pinching” and release in the hinge.

Thus, we conclude that the use of SLES concept in rotorcraft flight structure can cause serious problems with the resonances on the blades, as well as a significant increase in variable bending moments and loads on the blades.

6. CONCLUSION

According to the results of the research we can conclude that the developed method of calculation based on the forth integration of equations of rotor blades deformation is functional. It allows to obtain reliable results and study various concepts of rotorcraft flight structures associated with specific structural elements operating under all flight regimes, including unsteady ones.

7. REFERENCES

1. V.M. Pchelkin, N.S. Pavlenko,. Helicopter Main Rotor Head. Certificate of Authorship No. 1658538, 1991
2. Pavlenko N.S., A New Concept of the Main Rotor for a High-Speed Single-rotor Helicopter, Proceedings 33th European rotorcraft forum, Kazan, Russia, 2007
3. Pavlenko N.S., 400 km / h - Not the limit, "Helicopter industry", Moscow, December 2007
4. A.Y. Liss. The Study of the rotor in two planes bending, and torsion. Dissertation for the degree of Doctor of Technical Sciences, Kazan, 1974.
5. Averyanov I.O., Agamirov L.V., Ivchin V.A. The Study of the finite-difference scheme for calculating aircraft rotor strength for the transient and maneuver regimes. Scientific and Technical Conference "Gagarin Readings", 2010
6. Averyanov I.O., Ivchin V.A. Development of the calculation method for elastic rotor blade deformation in the plane of thrust, rotation and torsion by means of forth integration, Scientific Journal GA № 172, 2011

7. Averyanov I.O., Ivchin V.A. The Study of the rotor blade proper motion dynamics by the method of forth integration, Scientific Journal GA № 172, 2011
8. Mil M.L. and others, Helicopters, Vol.1, Moscow, Mechanical engineering, 1966
9. Aircraft Designer Directory, Vol.3, Strength of Aircraft, CAI, 1939
10. Ivchin V.A. Studies in the helicopter rotor control system load of transient flight regimes, Moscow, Mil, 1989
11. Averyanov I.O., Ivchin V.A. The Study of elastic rotor blade loads at "Gorka" maneuver by forth integration method, Scientific Journal GA № 177, 2011

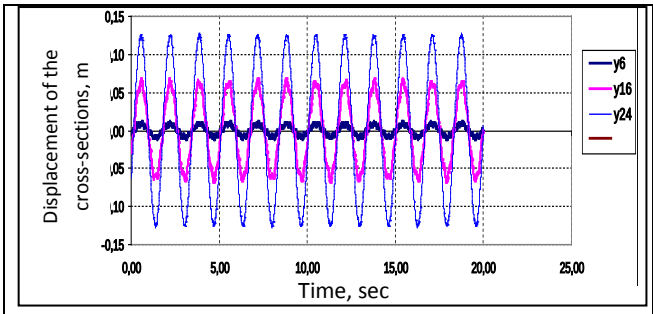

Figure 1. Results of analysis

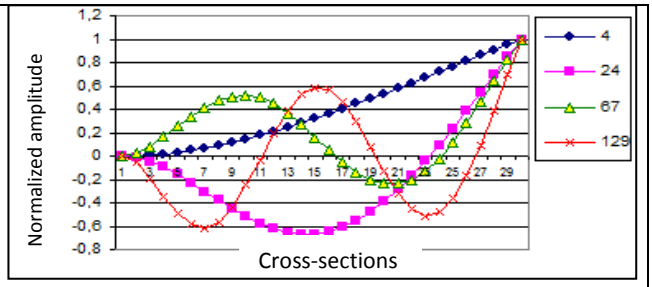

Figure 2. Natural forms and frequencies

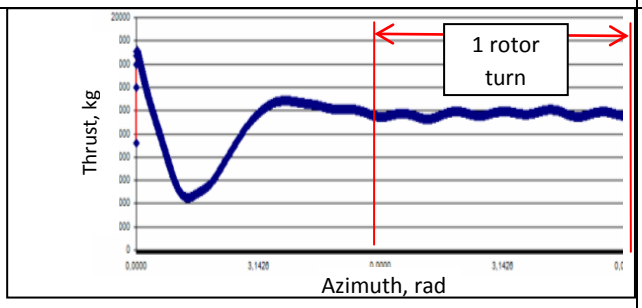

Figure 3. Regime "Horizontal flight". Rotor thrust

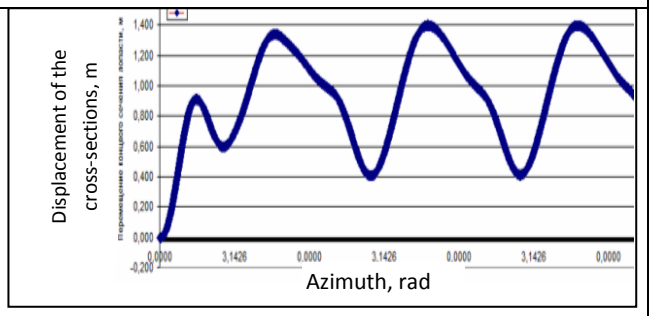

Figure 4. Regime "Horizontal flight". Displacement of the cross-section in vertical plane

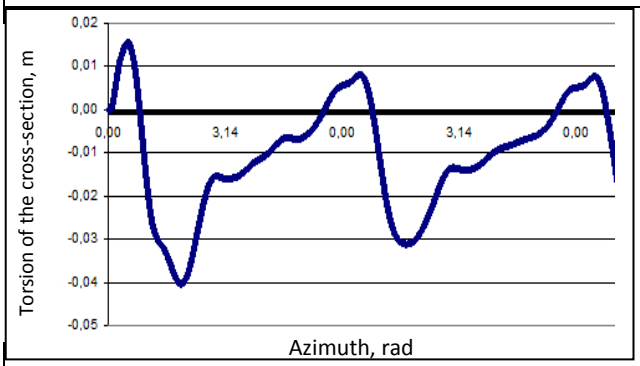

Figure 5. Regime "Horizontal flight". Displacement of the cross-section in a plane of blade turning

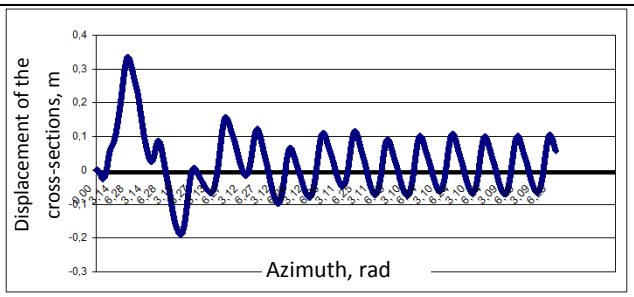

Figure 6. Regime "Horizontal flight". Displacement of the cross-section in plane of rotation of the blade

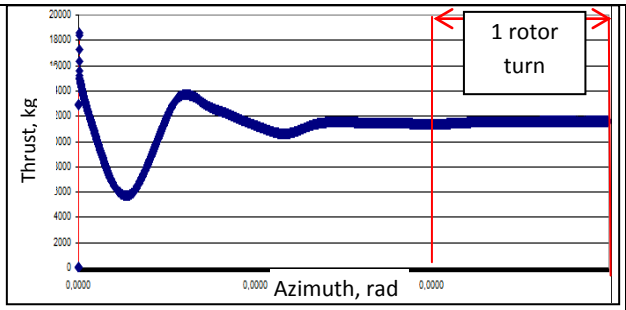

Figure 7. Regime "Hovering". Rotor thrust.

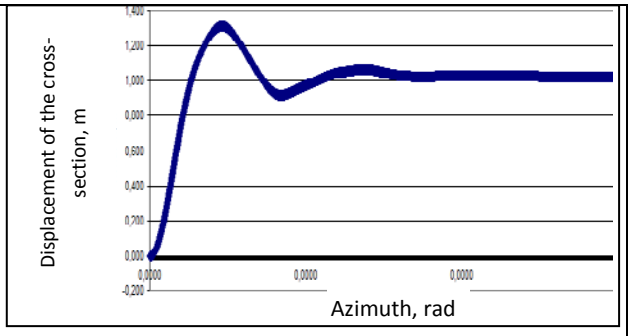

Figure 8. Regime "Hovering". Displacement of the cross-section in vertical plane

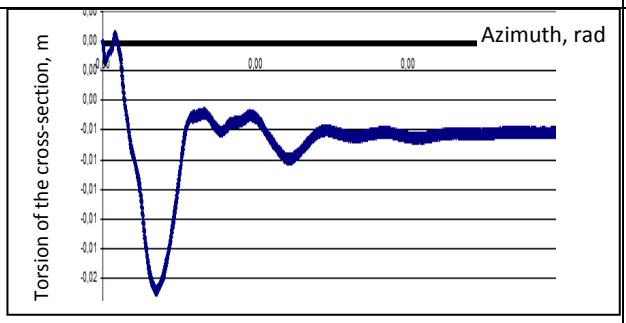

Figure 9. Regime "Hovering". Displacement of the cross-section in a plane of blade turning

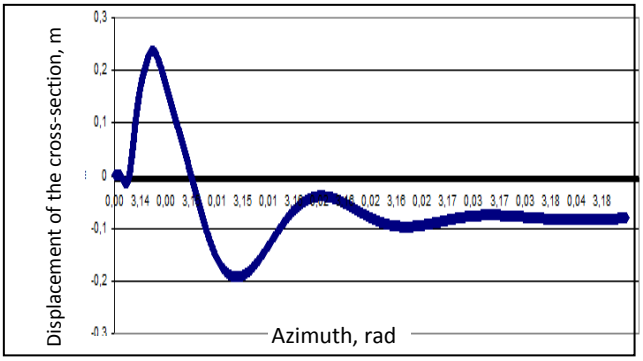

Figure 10. Regime "Hovering". Displacement of the cross-section in plane of rotation of the blade

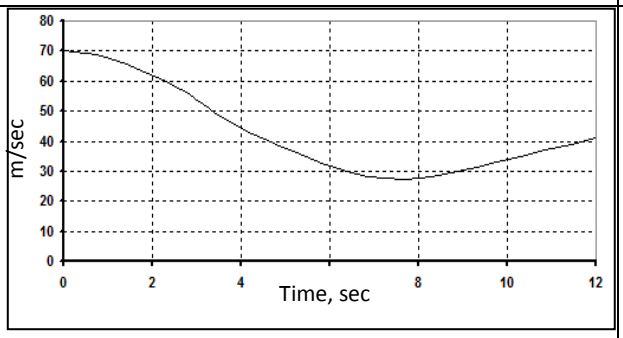

Figure 11. Speed changing during the maneuver

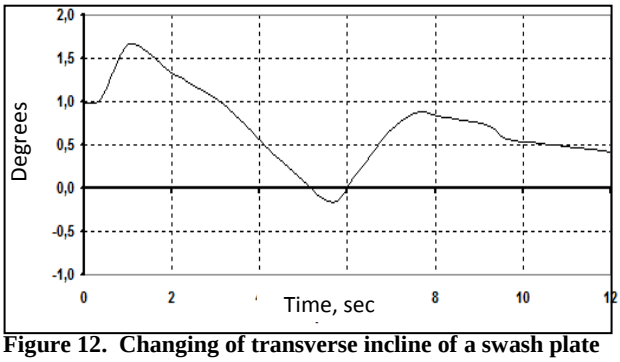

Figure 12. Changing of transverse incline of a swash plate during the maneuver

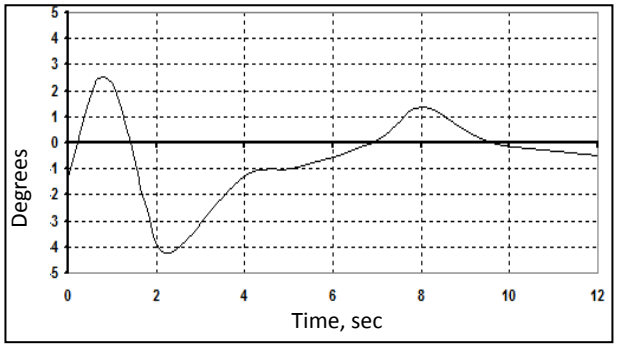

Figure 13. Changing of longitudinal incline of a swash plate during the maneuver

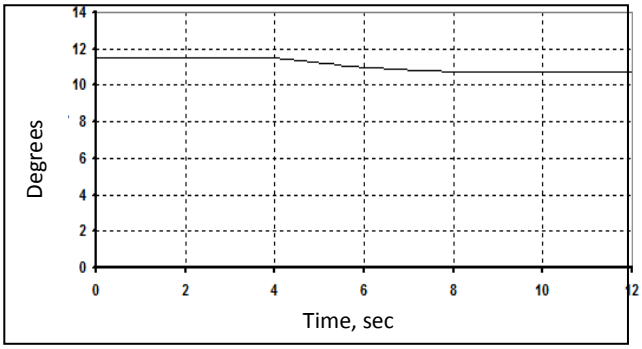

Figure 14. Changing of blade angle during the maneuver

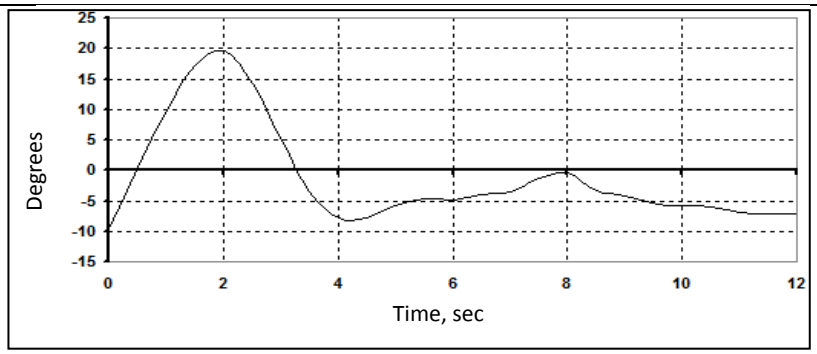

Figure 15. Changing of rotor angle of attack during the maneuver

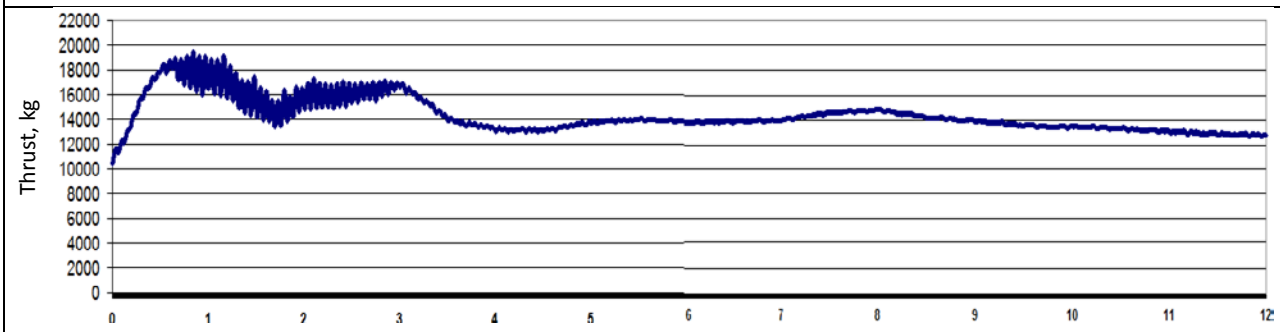

Figure 16. Rotor thrust changing during the maneuver

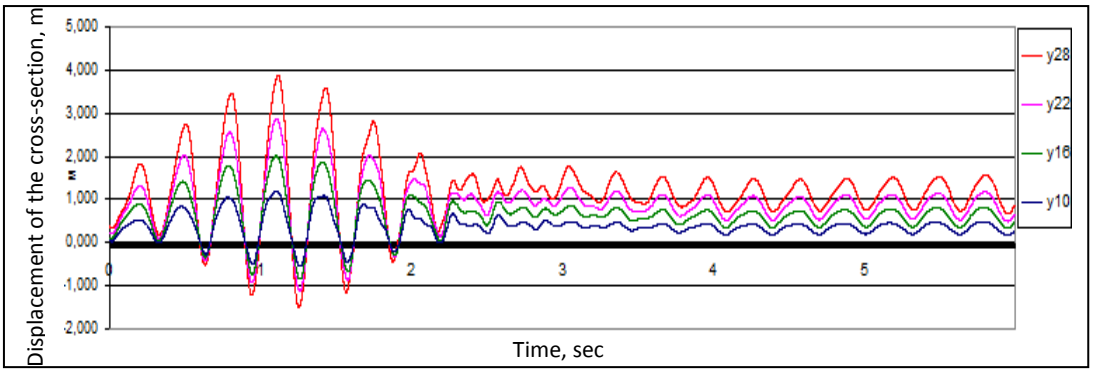

Figure 17. Displacement of cross-sections in vertical plane during the maneuver

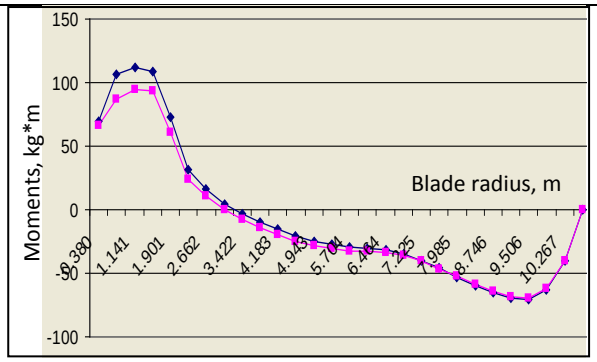

Figure 18. Distribution of constant bending moments in blade in its vertical plane during the maneuver

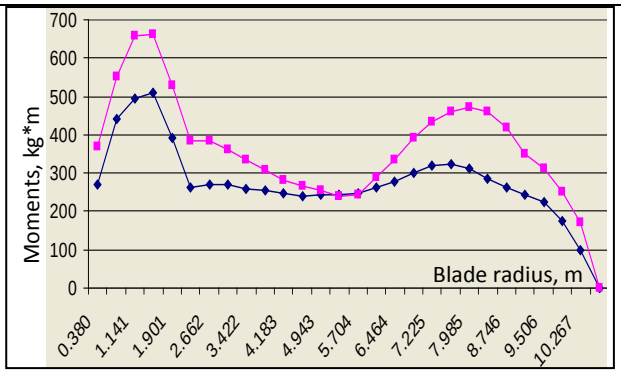

Figure 19. Distribution of changeable bending moments in blade in vertical plane during the maneuver

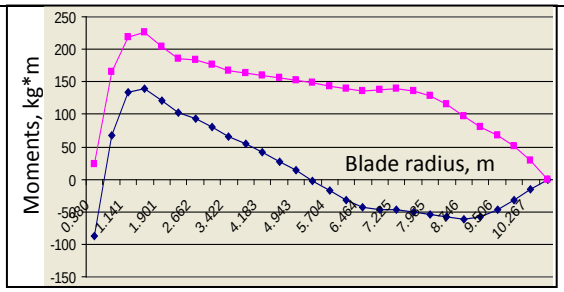

Figure 20. Distribution of constant bending moments in blade in rotation plane during the maneuver

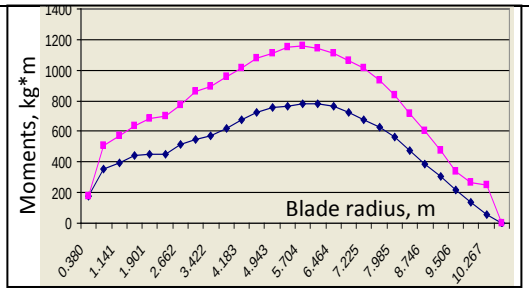

Figure 21. Distribution of changeable bending moments in blade in rotation plane during the maneuver

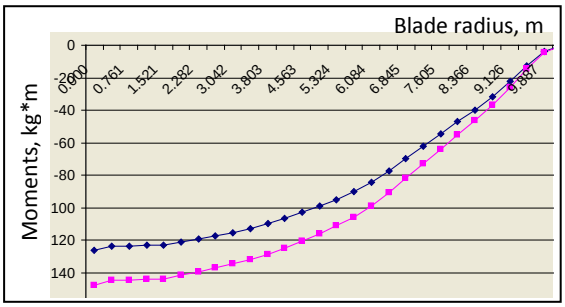

Figure 22. Distribution of constant torsion moments in blade during the maneuver

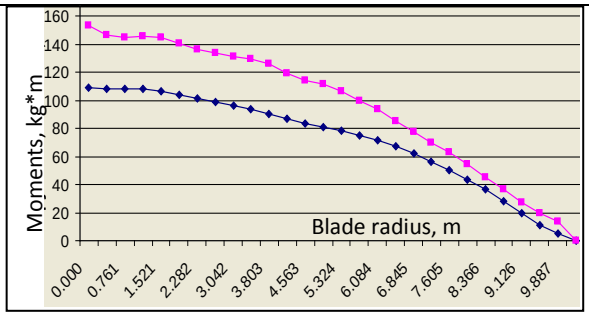

Figure 23. Distribution of changeable torsion moments in blade during the maneuver

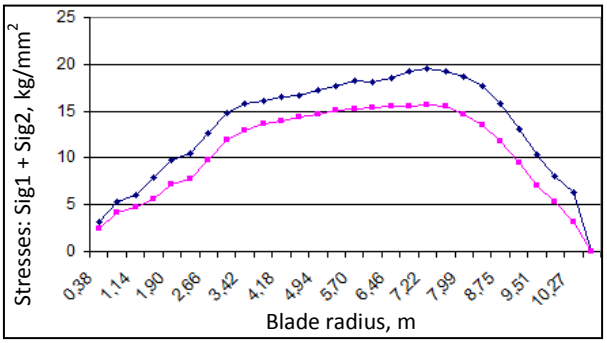

Figure 24. Distribution of equivalent bending stresses in blade during the maneuver

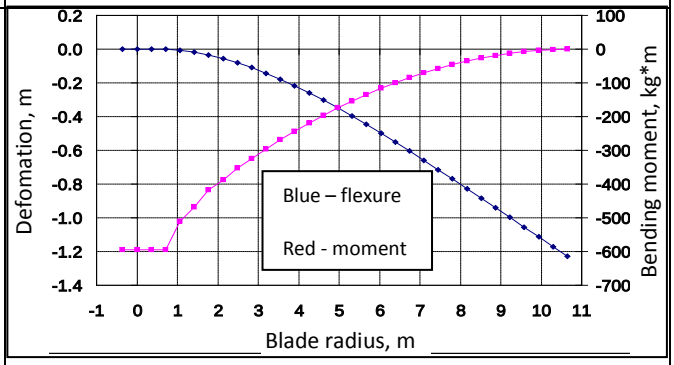

Figure 25. Static deformation of the blade

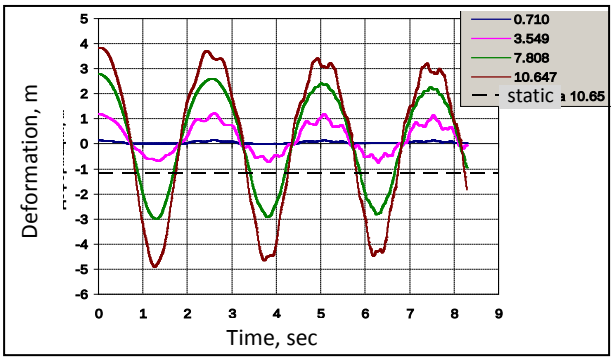

Figure 26. Displacement of cross-sections of the blade without damping

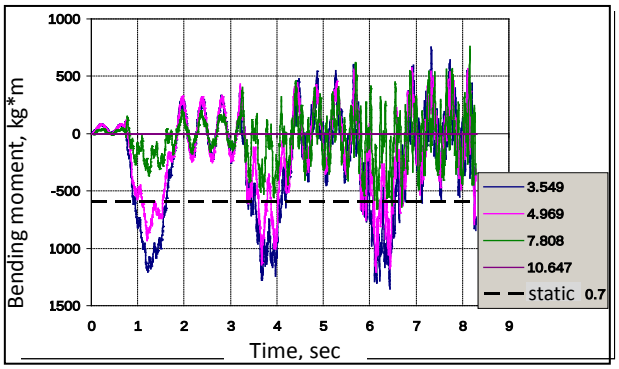

Figure 27. Bending moments for cross-sections of the blade without damping

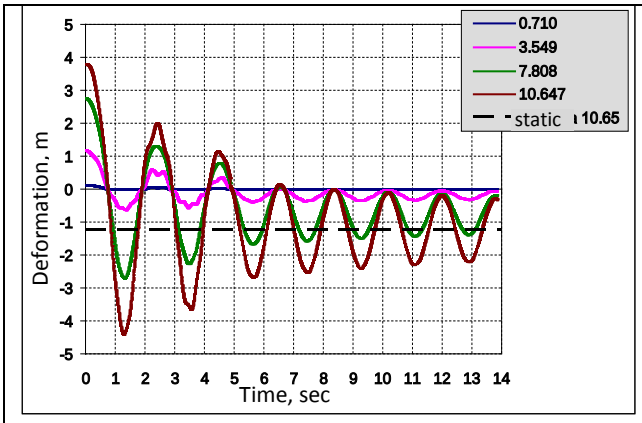

Figure 28. Displacement of cross-sections of the blade with damping

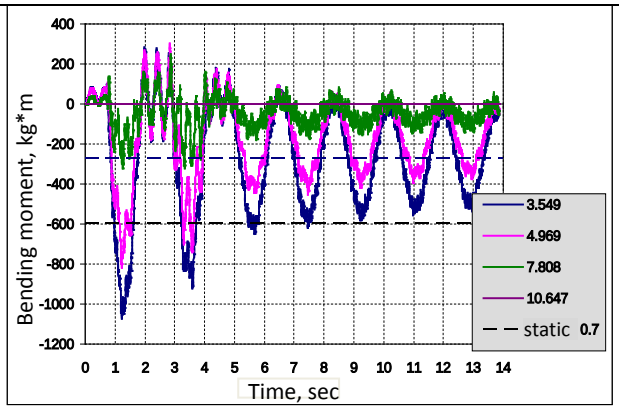

Figure 29. Bending moments for cross-sections of the blade with damping

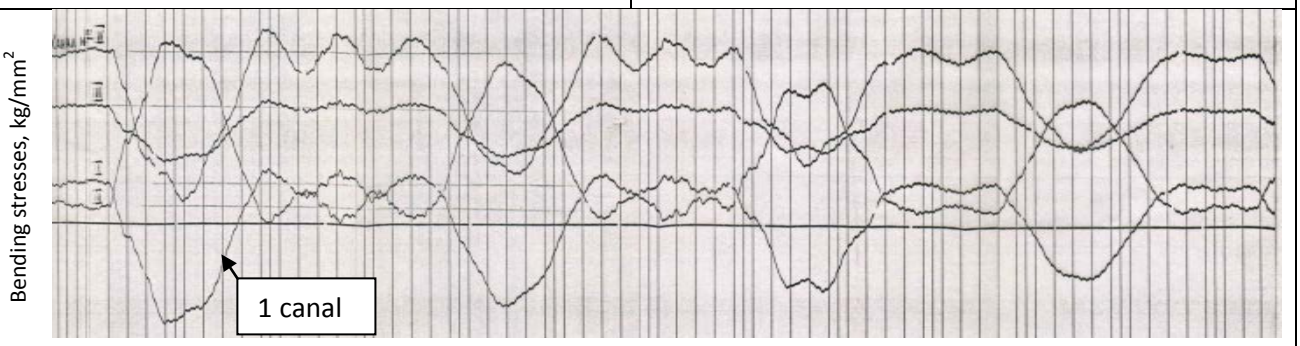

Figure 30. Test data. Bending stresses during the time

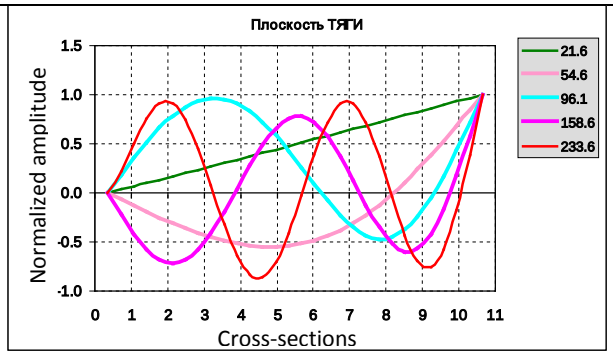

Figure 31. Natural forms and frequencies of hinged blade. Vertical plane

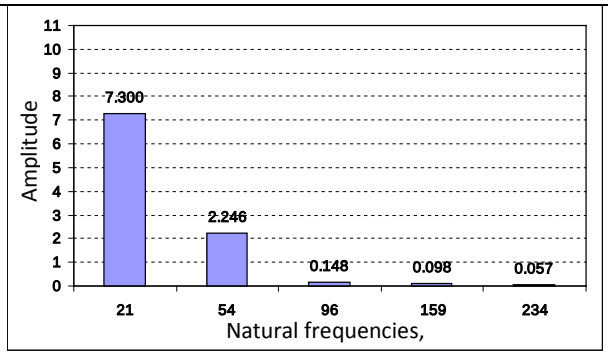

Figure 32. Natural frequencies contribution

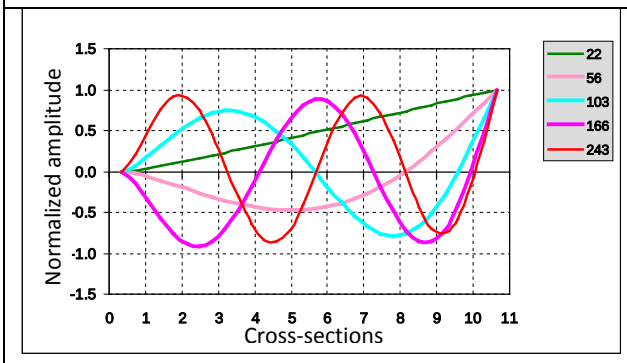

Figure 33. Natural forms and frequencies of rigidly clamped blade. Vertical plane

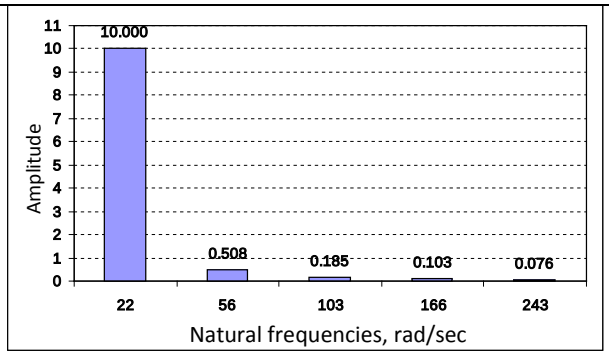

Figure 34. Natural frequencies contribution

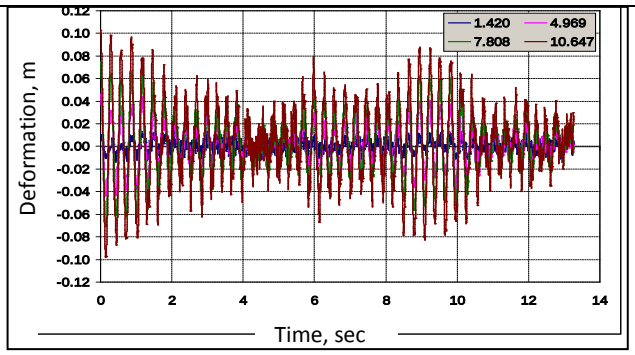

Figure 35. Deformations of the blade cross-sections in SLES. Locked in 225-315 degree

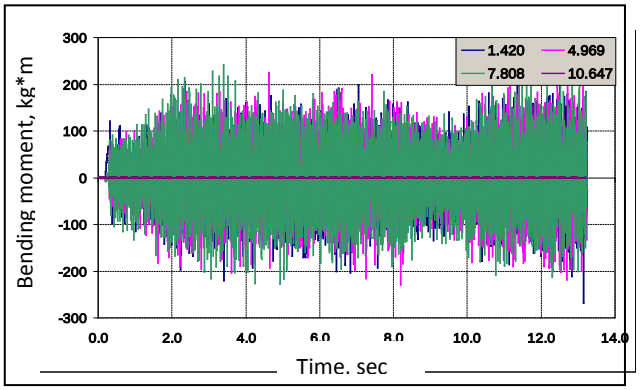

Figure 36. Bending moments of the blade cross-sections in SLES. Locked in 225-315 degree

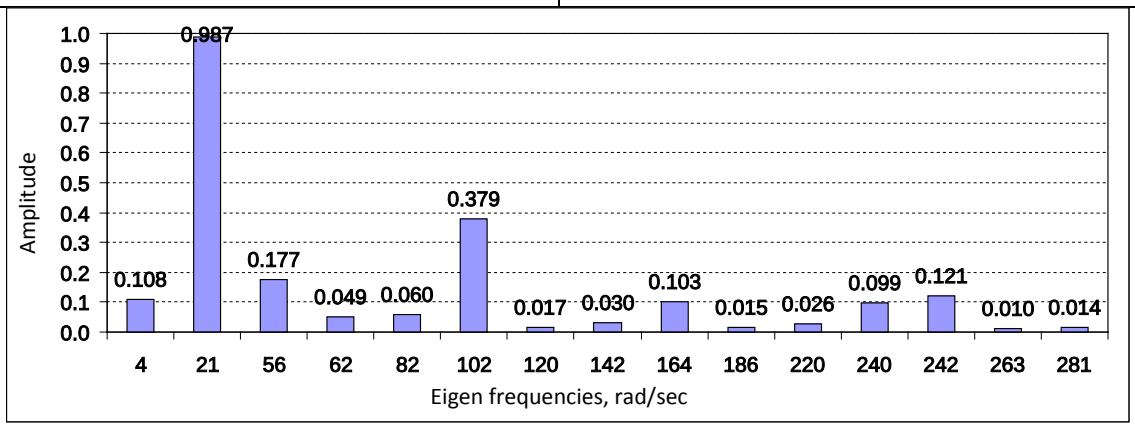

Figure 37. Natural frequencies contribution in SLES. Locked in 225-315 degree

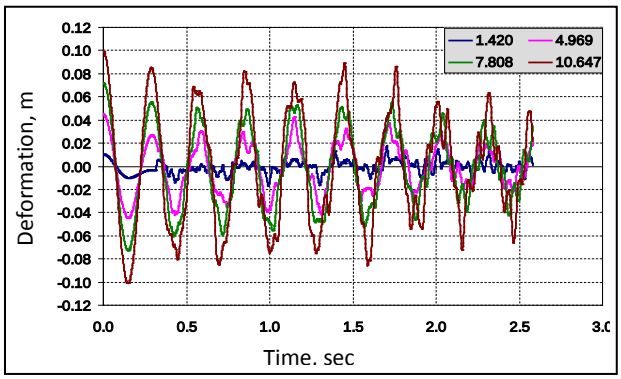

Figure 38. Deformations of the blade cross-sections in SLES. Locked in 180-360 degree

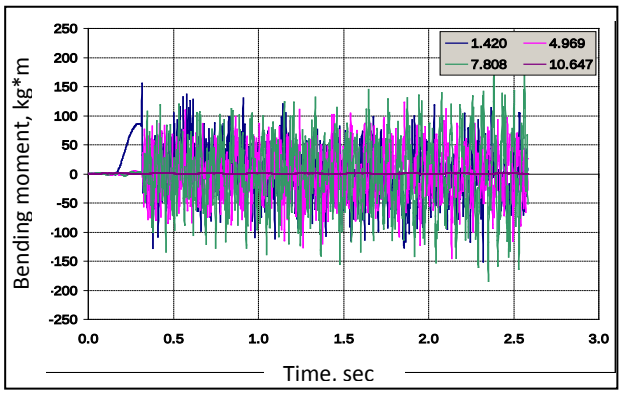

Figure 39. Bending moments of the blade cross-sections in SLES. Locked in 180-360 degree